ChemComm

Accepted Manuscript

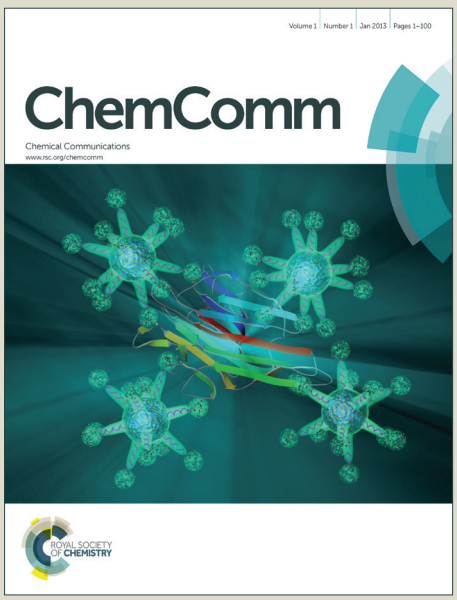

ROYAL SOCIETY OF CHEMISTRY

www.rsc.org/chemcomm

Journal Name

RSCPublishing

COMMUNICATION

Plasmonic properties of triangle-shaped silver trimers selectively fabricated by near-field photo-reduction using an apertured cantilever for an atomic force microscope

Yasutaka Kitahama,[a] Takuya Ikemachi,[a] Toshiaki Suzuki,[a] Takeshi Miura[b] and Yukihiro Ozaki[a]

Cite this: DOI: 10.1039/x0xx00000x

Received 00th January 2012,
Accepted 00th January 2012

DOI: 10.1039/x0xx00000x

www.rsc.org/

On an $AgNO_3$ crystal, an equilateral or right-angle triangle-shaped Ag trimer was selectively fabricated through near-field photo-reduction and observed *in situ* by using an apertured cantilever coupled with an atomic force microscope. By using the different triangle-shaped Ag trimers, irradiation wavelength and polarization dependence of surface-enhanced Raman scattering were investigated.

Recently, nanostructures have been widely applied. Also in the field of "plasmonics" such as surface-enhanced spectroscopy and plasmon-enhanced photo reaction, various kinds of noble metal nanostructures have been proposed;[1,2] for example, electrodes roughened by oxidation-reduction cycles, metal colloids prepared by reducing a metal ion in an aqueous solution, and nanoblocks produced by lithography and vapor deposition. It is important to control the size and shape of the nanostructure, because an enhanced electromagnetic (EM) field on the metallic nanostructure is influenced by them.[1,2] The enhanced EM field is induced by resonance of plasmon due to the dipolar oscillation of the conduction band electrons on the metallic nanostructure with incident light, which is called as localized surface plasmon resonance (LSPR).[1,2] At a junction of the nanostructure, the EM field is enormously enhanced, and then it causes surface-enhanced spectroscopy and plasmon-enhanced photo reaction of molecule adsorbed on the metal. Indeed, surface-enhanced Raman scattering (SERS) is increased by the irradiation light polarized parallel to the long axis of a dimer of noble metal nanoparticles.[3–5]

In the previous studies of plasmon using lithography and vapor deposition,[2,6–9] the metallic substrate usually consists of only specific sized, shaped, and arranged nanostructures. On the other hand, metal nanoparticles in the colloidal dispersion show various sizes, shapes, and arrangements.[2–5,10–15] Colloidal nanoparticles have been used for the studies of SERS mechanism; for example, the relation among LSPR, SERS, and shape of the nanoparticles has been investigated by a conventional microspectroscopy and a scanning or transmission electron microscope (SEM or TEM).[4,10,15] Furthermore, arrangement of the colloidal nanoparticles and the EM field around the nanoparticles have been observed simultaneously by using a scanning near-field optical microscope (SNOM),[5] in which incident light passes through a small aperture whose size is smaller than the wavelength of the light and changes into a near-field light at the aperture. However, it is difficult to select desired shape, size, and arrangement of the nanoparticles.

In the present study, a metallic nanostructure was fabricated on an $AgNO_3$ crystal by near-field photo-reduction using an apertured cantilever coupled with an atomic force microscope (AFM), which was used for a near-field infrared and Raman imaging.[16] The near-field illumination area is defined by dimension of the aperture. When the aperture approaches a sample, the near-field light interacts with the sample inside the dimension, and thus it can reduce a metal ion to the metal.[17] Conventional photo-reduction of a metal ion at a laser focal area has already been reported as on-demand synthesis of metallic SERS-active nanoparticles.[18] In our system, the near-field photo-reduced nanostructure can be selectively fabricated and observed by the same apertured cantilever coupled with the AFM immediately after the near-field photo-reduction, namely, *in situ* AFM observation. We formed a third Ag nanoparticle at slightly different position beside an Ag dimer, and then an equilateral or right-angle triangle-shaped (V- or L-shaped) Ag trimer was selectively fabricated by the near-field photo-reduction as compared with the previous fabrication.[8,11–15] By using the different triangle-shaped trimers, irradiation wavelength and polarization dependence of SERS of 4,4'-bipyridine molecules adsorbed on them were investigated.

The near-field photo-reduction was performed by an AFM setup which is combined with a reflection mode Raman microscope (Photon design, Nanostar NFRSM800). The apertured cantilever, made by UNISOKU, was attached to a quartz tuning fork of a shear-force-based AFM. For the near-field photo-reduction, the 514 nm line from an Ar ion laser (Spectra Physics, Stabilite 2017-06S) was used. The laser beam (5 mW) was focused onto an $AgNO_3$ crystal through the aperture of the cantilever (200 nm in diameter; see Fig. S1 in ESI) by an objective lens with a long working distance (90×, NA = 0.71) for 300 s. After the near-field photo-reduction, topographic images of the crystal surface were observed by the same apertured cantilever coupled with the AFM. Then, 4,4'-bipyridine in acetone (100 mM) was dropped on the crystal. After evaporation, a SERS spectrum was measured by irradiation of a defocused beam of the same Ar ion laser (λ = 514 nm, 0.1 mW) or a solid-state laser

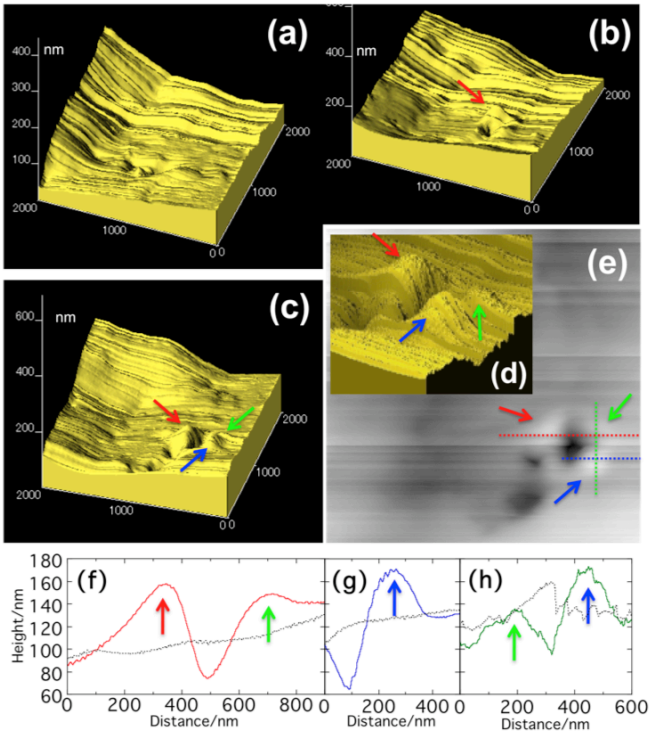

Fig. 1 3D AFM images of the same crystal surface of $AgNO_3$ (a,b) during and (c,d) after near-field photo-reduction. (d) The enlargement of (c), which is slightly rotated. (e) 2D AFM image, which covers 2 × 2 μm^2, of the near-field photo-reduced trimer. Height trace analysis of the (f) red, (g) blue, and (h) yellow-green dotted lines in (e). In (f-h), the black dotted curves show heights of the nearby surface without the near-field photo-reduction.

(CrystaLaser, DL638-025-S; λ = 640 nm, 3 mW) onto the crystal not through the apertured cantilever, but through the objective lens. Polarized irradiation and SERS light was rotated and depolarized by λ/2 and λ/4 plates, respectively.

Fig. 1 shows AFM images of surfaces of crystalline $AgNO_3$ immediately after near-field photo-reduction (see also Fig. S2 in ESI). Reaction pathway of the photo-reduction,[19] which is promoted by traces of organic matter, is given by

$$2AgNO_3 \rightarrow 2Ag + 2NO_2 \uparrow + O_2 \uparrow .$$

The photo-reduced diatomic silver is hardly re-oxidized.[20] Before near-field photo-reduction, a smooth surface was observed (see also Fig. S2 in ESI). Fig. 1d–1h show that not two, but three nanostructures were formed by three times shifts of the near-field photo-reduction point and observed in the lower right areas of the AFM images. The third nanostructure can be arranged at a desired position by the near-field photo-reduction, although the conventional photo-reduction forms only a single or many metallic nanoparticles on a glass in a solution containing the metal salt.[18] Thus, we selectively fabricated various triangle-shaped trimers such as V- and L-shaped triangles. Because it is difficult to find the position due to a change of the apparatus, we could not observe the near-field photo-reduced nanostructures by a SEM or changing to a conventional AFM cantilever. On the other hand, not only the final result, but also the progress can be observed by the same apertured cantilever.

Fig. 2 shows Raman spectra of 4,4'-bipyridine on the $AgNO_3$ crystal after and before the near-field photo-reduction. These spectra were normalized by the intensity of a strong peak at 1045 cm^{-1}, which is attributed to the symmetrical stretching mode of nitrate ion.[21,22] The condition of Raman measurement such as an exposure time was regulated to prevent photo-degradation of the sample at a

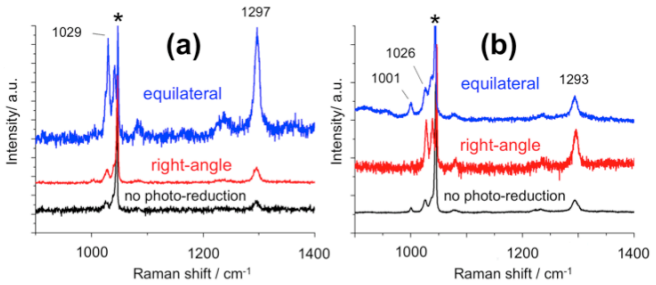

Fig. 2 SERS spectra of 4,4'-bipyridine from the V and L-shaped Ag trimers on a $AgNO_3$ crystal and Raman spectra of that before the near-field photo-reduction. These spectra were measured by the irradiation at (a) 514 and (b) 640 nm. The asterisked peaks are due to nitrate ion in the crystal.

solid-gas interface. Thus their signal to noise ratios were different. After the near-field photo-reduction, the Raman spectra were enhanced. Therefore, the near-field photo-reduced trimers may be composed of metallic silver, although it is difficult to determine the elemental composition even by X-ray photoelectron spectroscopy due to small shifts in binding energy for the silver ion state compared with the metallic state.[23] However, these SERS spectra were not so much enhanced. The reason is that the concentrated sample was used to be uniformly adsorbed on junctions and surface of the Ag nanoparticles, and conventional photo-reduction was induced by the irradiation light for measurement of the spectra. The Raman peaks around at 1000 and 1030 cm^{-1} are assigned to the ring-breathing mode of polycrystalline 4,4'-bipyridine and the metal complex, respectively.[24] The Raman peak around at 1295 cm^{-1} is attributed to the inter ring stretch mode of 4,4'-bipyridine.[24] In the lower wavenumber side of the peak at 1045 cm^{-1}, the shoulder or peak appears at 1039 cm^{-1} and is assignable to the symmetrical stretching mode of nitrate ion at 175 ºC.[21] From the V-shaped triangle, the SERS by the irradiation at 514 nm was about 3.8 times stronger than that at 640 nm (see the top spectra in Fig. 2a and 2b). It is noted that the irradiation wavelength dependence was contrary to the results from the L-shaped triangle, from which the SERS by the irradiation at 514 nm was about 0.3 times stronger than that at 640 nm (see the middle spectra in Fig. 2a and 2b).

To explore the contrary results, we calculated plasmon resonance scattering spectra from the triangles and the spatial distribution of the enhanced EM field around the triangles. Fig. 3a shows the calculated back-scattering spectra from V- and isosceles L-shaped trimer that consists of Ag nanoparticles of 200 nm in diameter, which is the same size as the aperture of the cantilever, by a finite-difference time-domain (FDTD) method. The polarization direction of the irradiation light was along the closest long axis of the dimer in the trimer (horizontally in Fig. 3b–3d and 0° in the inset of Fig. 4b), which is similar to the experimental conditions. In the case of the V-shaped triangle, three bands appear around at 710, 600, and 490 nm. The former bands are similar to those in the previous paper,[8] in which the band around at 650 nm has been split by approach of component Ag discs of V-shaped triangle, and then the blue- and red-shifted bands have appeared. In the current result, also the prominent peak appears at 490 nm (the previous spectra were displayed in the range from 500 to 900 nm)[8] and may be due to coupling of multipolar surface plasmon resonance.[25] Fig. 3b–3d display the EM fields around the V-shaped triangles by the irradiation at 490, 600, and 710 nm, respectively. By the irradiation at 600 nm, the enhanced EM field is displayed only at the junction of the dimer along the polarization. On the other hand, the enhanced EM field appears also at the gaps between the dimer along the polarization and the third Ag particle irradiated at 490 and 710 nm.

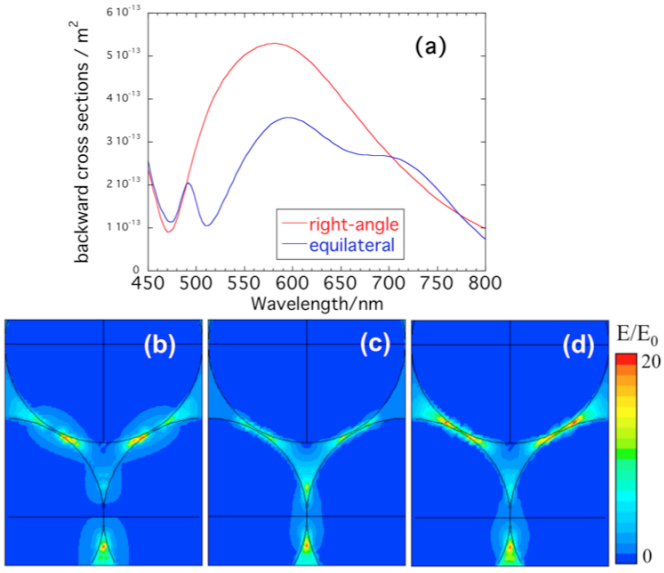

Fig. 3 (a) Calculated back-scattering spectra from the L and V-shaped Ag trimers that consist of Ag particles of 200 nm in diameter. Calculated spatial distribution of the enhanced electromagnetic field around the V-shaped Ag trimer irradiated by the horizontal polarization at (b) 490, (c) 600, and (d) 710 nm. The images cover 200 × 250 nm^2.

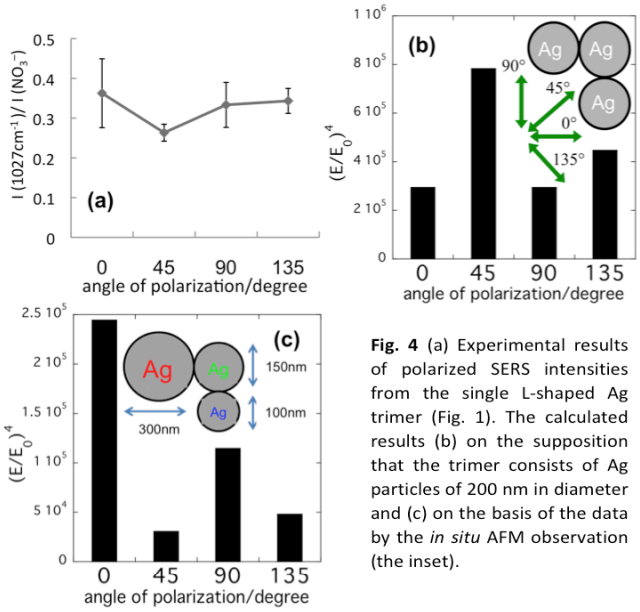

Fig. 4 (a) Experimental results of polarized SERS intensities from the single L-shaped Ag trimer (Fig. 1). The calculated results (b) on the supposition that the trimer consists of Ag particles of 200 nm in diameter and (c) on the basis of the data by the *in situ* AFM observation (the inset).

For the isosceles L-shaped triangle, the monotonous back-scattering band is derived around at 580 nm by calculation, and the third Ag particle not beside two, but beside one particle may scarcely interact with the EM field around the component dimer like Fig. 3c (λ = 600 nm).

From the calculated spectra, the experimental excitation wavelength dependence can be interpreted as follows. By the irradiation at 514 nm, the V-shaped triangle can emit SERS more strongly than that at 640 nm, because the irradiation wavelength at 514 nm is closer to the resonance band at 490 nm, although the valley between the resonance bands at 600 and 710 nm exists at 640 nm. Even if the irradiation wavelength at 640 nm is close to the resonance band at 600 nm due to the red-shifted spectrum on the experimental condition, the enhanced EM field appears not at three, but at one junction. In the case of the isosceles L-shaped triangle, the irradiation wavelength at 640 nm is closer to the resonance band at 580 nm than that at 514 nm. Therefore, the SERS from the V- and L-shaped triangles were measured more strongly by the irradiation at 514 and 640 nm, respectively.

The polarization dependence of the triangle-shaped Ag trimer is also investigated. In the case of the V-shaped triangles, the polarization-independent response has been reported.[8,12–14] Thus, the polarization dependence of SERS from the L-shaped triangle in Fig. 1c were measured by the irradiation at 514 nm. Fig. 4a shows the experimental SERS intensities at each angle of the polarization direction of the irradiation light. The intensities of the SERS are those of the peak due to the ring breathing mode of 4,4'-bipyridine (1027 cm^{-1}) normalized by those due to the symmetrical stretching mode of the nitrate ion in the crystal (the spectra are shown in Fig. S3 in ESI).[21,22,24] To derive the SERS intensity by the FDTD calculation, we sum up the fourth power of the maxima of the EM field, which appear at the junctions (see Fig. S4 in ESI), because SERS enhancement factor is proportional to the fourth power of EM field due to two-fold enhancement of SERS.[26] Thus, the maximum EM field nearly contributes to the SERS intensity. Fig. 4b shows the calculated results of the polarized SERS intensities on the supposition that the trimer consists of Ag particles of 200 nm in diameter, which is the same size as the aperture of the cantilever. The calculated result for the isosceles L-shaped triangle represents that the SERS by the polarization (λ = 514 nm) at an angle of 45° is stronger than that of 135°, which is consistent with the previous paper,[13] and the weakest SERS is emitted by the polarization at an angle of 0 and 90°. However, these are different from the experimental results (Fig. 4a).

Then, we calculated the polarized SERS intensities again on the basis of the data by the *in situ* AFM observation in Fig. 1. The diameters of the Ag nanoparticles were roughly estimated to be 300, 150 and 100 nm by subtracting the aperture size of the cantilever (200 nm) from the distance between the minimum points in Fig. 1f–1h (Fig. 1h shows the noisy curves, because the traces are perpendicular to the scanning direction). The spatial resolution may be improved by using an apertured cantilever whose tip is diagonally cut. These different sized nanostructures may be caused by the inhomogeneity on the polycrystalline surface of $AgNO_3$. The arrangement is illustrated in the inset of Fig. 4c. The calculation for the scalene L-shaped triangle reproduces the experimental results better as shown in Fig. 4c. The improvement can be explained by the enhanced EM field images around the L-shaped triangles (see Fig. S4 in ESI). In the case of the isosceles L-shaped triangle, the enhancement takes place at two junctions of the equivalent component dimers irradiated by the polarization (λ = 514 nm) at an angle of 45 and 135°. On the other hand, the maximum EM field appears only at one junction of the smallest dimer in the scalene L-shaped trimer. Therefore, the calculated SERS from the scalene L-shaped triangle as the experimental results is derived to be stronger by the polarization at an angle of 0 and 90° than that of 45 and 135° (Fig. 4c), although the calculated results for the isosceles L-shaped triangle are opposite (Fig. 4b).

In summary, the near-field photo-reduced V- or L-shaped Ag trimer was selectively fabricated on an $AgNO_3$ crystal and observed *in situ* by the apertured cantilever coupled with AFM. By the irradiation at 514 and 640 nm, the wavelength dependence of SERS from the V-shaped triangle was contrary to that from the L-shaped triangle. The difference is induced by their back-scattering spectra, in which the resonance bands of the V- and L-shaped triangles are calculated to be around at 490, 600, 710 nm, and 580 nm, respectively. The bands at 490 and 710 nm originate from the EM

interaction between the third Ag particle and the dimer in the V-shaped triangle. By the polarization (λ = 514 nm) at an angle of 45°, the SERS from the L-shaped triangle was measured most weakly, although the SERS from the isosceles L-shaped triangle is derived to be weakest by the calculation using that of 0 and 90°. On the basis of the data by the *in situ* AFM observation, we calculated again and then reproduced the experimental polarization dependence better. Thus, this method will be very useful for trial productions of plasmonic devices, because not only various arranged but also various sized and shaped metal nanostructures (rods, crescents, rings, and so on) can be fabricated easily by near-field photo-reduction while scanning and *in situ* observed topographically by the same AFM.

This work was supported by KAKENHI (No. 23750025, 25410029) and a Support Project to Assist Private Universities in Developing Bases for Research (Research Center for Single Molecule Vibrational Spectroscopy) from the Ministry of Education, Culture, Sports, Science and Technology of Japan.

Notes and references

[a] *Department of Chemistry, School of Science and Technology, Kwansei Gakuin University, Sanda, Hyogo 669-1337, Japan. E-mail: kitahama@kwansei.ac.jp; Fax: +81-79-565-9077; Tel: +81-79-565-8349.*
[b] *UNISOKU Co. Ltd., 2-4-3 Kasugano, Hirakata, Osaka 573-0131, Japan.*

† Electronic Supplementary Information (ESI) available: SEM image of the apertured cantilever; AFM images of crystal surface of $AgNO_3$ before and after the near-field photo-reduction; Polarized SERS spectra from the single L-shaped Ag trimer; Calculated spatial distribution of EM fields around the L-shaped Ag trimers. See DOI: 10.1039/c000000x/

1 (*a*) Y. Ozaki, K. Kneipp and R. Aroca, *Frontiers of surface-enhanced Raman scattering*, John Wiley & Sons Ltd., Chichester, 2014; (*b*) E. C. Le Ru and P. G. Etchegoin, *Principles of surface-enhanced Raman spectroscopy and related plasmonic effects*, Elsevier, Amsterdam, 2009; (*c*) K. Kneipp, M. Moskovits and H. Kneipp, *Surface-Enhanced Raman Scattering –Physics and Applications,* Springer, Heidelberg and Berlin, 2006; (*d*) R. Aroca*, Surface-Enhanced Vibrational Spectroscopy*, John Wiley & Sons Ltd., Chichester, 2006.
2 (*a*) G. A. Baker and D. S. Moore, *Anal. Bioanal. Chem.,* 2005, **382**, 1751; (*b*) S. Lal, N. K. Grady, J. Kundu, C. S. Levin, J. B. Lassiter and N. J. Halas, *Chem. Soc. Rev.,* 2008, **37**, 898.
3 T. Itoh, Y. Kikkawa, K. Yoshida, K. Hashimoto, V. Biju, M. Ishikawa and Y. Ozaki, *J. Photochem. Photobiol. A,* 2006, **183**, 322.
4 K. Yoshida, T. Itoh, H. Tamaru, V. Biju, M. Ishikawa and Y. Ozaki, *Phys. Rev. B,* 2010, **81**, 115406.
5 K. Imura, H. Okamoto, M. K. Hossain and M. Kitajima, *Nano Lett.,* 2006, **6**, 2173.
6 C. L. Haynes and R. P. Van Duyne, *Nano Lett.,* 2003, **3**, 939.
7 M. Takase, Y. Sawai, H. Nabika and K. Murakoshi, *J. Photochem. Photobiol. A,* 2011, **221**, 169.
8 J. Alegret, T. Rindzevicius, T. Pakizeh, Y. Alaverdyan, L. Gunnarsson and M. Käll, *J. Phys. Chem. C,* 2008, **112**, 14313.
9 L. Gunnarsson, T. Rindzevicius, J. Prikulis, B. Kasemo, M. Käll, S. Zou and G. C. Schatz, *J. Phys. Chem. B,* 2005, **109**, 1079.
10 J. P. Camden, J. A. Dieringer, Y. Wang, D. J. Masiello, L. D. Marks, G. C. Schatz and R. P. Van Duyne, *J. Am. Chem. Soc.,* 2008, **130**, 12616.
11 K. L. Wustholz, A. -I. Henry, J. M. McMahon, R. G. Freeman, N. Valley, M. E. Piotti, M. J. Natan, G. C. Schatz and R. P. Van Duyne, *J. Am. Chem. Soc.,* 2010, **132**, 10903.
12 D. Steinigeweg, M. Schütz and S. Schlücker, *Nanoscale,* 2013, **5**, 110.
13 L. Chuntonov and G. Haran, *Nano Lett.,* 2011, **11**, 2440.
14 L. Chuntonov and G. Haran, *J. Phys. Chem. C,* 2011, **115**, 19488.
15 K. Yoshida, T. Itoh, H. Tamaru, V. Biju, M. Ishikawa and Y. Ozaki, *Phys. Rev. B,* 2010, **81**, 115406.
16 (*a*) T. Masaki, K. Goto, T. Inouye and S. Kawata, *J. Appl. Phys.,* 2004, **95**, 334; (*b*) A. Sakai, N. Sasaki, T. Tamate and T. Ninomiya, *Ferroelectrics,* 2003, **284**, 15.
17 Y. Kitahama, T. Itoh, J. Aoyama, K. Nishikata and Y. Ozaki, *Chem. Commun.,* 2009, 6563.
18 (*a*) E. J. Bjerneld, F. Svedberg and M. Käll, *Nano Lett.,* 2003, **3**, 593; (*b*) M. V. Cañamares, J. V. Garcia-Ramos, J. D. Gómez-Verga, C. Domingo and S. Sanchez-Cortes, *Langmuir*, 2007, **23**, 5210; (*c*) Y. Kitahama, T. Itoh, T. Ishido, K. Hirano and M. Ishikawa, *Bull. Chem. Soc. Jpn.,* 2011, **84**, 976; (*d*) T. Itoh, V. Biju, M. Ishikawa, S. Ito and H. Miyasaka, *Appl. Phys. Lett.,* 2009, **94**, 144105.
19 Y. -H. Lin, K. -T. Chen and J. -R. Ho, *Jpn. J. Appl. Phys.,* 2011, **50**, 065002.
20 T. Tani, *Photographic Science*, Oxford University Press, New York, 2011.
21 K. Balasubrahmanyam and G. J. Janz, *J. Chem. Phys*., 1972, **57**, 4084.
22 Z. Zhou, G. G. Huang and Y. Ozaki, *Chem. Lett.,* 2010, **39**, 1203.
23 V. K. Kaushik, *J. Electron Spectrosc. Relat. Phenom.,* 1991, **56**, 273.
24 (*a*) M. Suzuki, Y. Niidome and S. Yamada, *Thin Solid Films,* 2006, **496**, 740; (*b*) S. -W. Joo, *Vib. Spectrosc.,* 2004, **34**, 269.
25 (*a*) Y. Tanaka, A. Sanada and K. Sasaki, *Sci. Rep.,* 2012, **2**, 764; (*b*) Y. Kitahama, A. Enogaki, Y. Tanaka, T. Itoh and Y. Ozaki, *J. Phys. Chem. C,* 2013, **117**, 9397.
26 (*a*) T. Itoh, K. Yoshida, V. Biju, Y. Kikkawa, M. Ishikawa and Y. Ozaki, *Phys. Rev. B,* 2007, **76**, 085405; (*b*) K. Yoshida, T. Itoh, V. Biju, M. Ishikawa and Y. Ozaki, *Phys. Rev. B,* 2009, **79**, 085419.

